Energy, Mines and Resources Canada | Énergie, Mines et Ressources Canada

CANMET

Canada Centre for Mineral and Energy Technology | Centre canadien de la technologie des minéraux et de l'énergie

PYROLYSIS OF PITCH DERIVED FROM HYDROCRACKED ATHABASCA BITUMEN

M.V. CHANDRA SEKHAR AND M. TERNAN

CATALYSIS SECTION

SYNTHETIC FUELS RESEARCH LABORATORY

OCTOBER 1977

ENERGY RESEARCH PROGRAM

ENERGY RESEARCH LABORATORIES

REPORT ERP/ERL 77-94 (J)

SUMMARY

Results of isothermal and temperature programmed pyrolysis experiments in an inert atmosphere and at temperatures from 350°C to 1000°C are presented. Thermogravimetric techniques using a recording microbalance were employed for following the weight changes occuring during the pyrolysis. Several techniques including ^{13}C n.m.r., gas chromatography, mass spectrometry and standard ASTM methods were used to analyze the decomposition products and the unreactive char. The bulk of the weight loss, as much as 35% by weight of the original sample, occurs at temperatures below 500°C. The mechanism of pyrolysis can be adequately described as proceeding in two stages. During the first stage, when about 20% of the sample decomposes, the pyrolytic reactions follow overall first order kinetics. During this stage the activation energy and the pre-exponential factor both increase with increasing extent of reaction and exhibit a kinetic compensation effect. During the remainder of the pyrolysis, the activation energy decreases with increasing extent of reaction and the kinetics become complex.

PYROLYSIS OF PITCH DERIVED FROM HYDROCRACKED ATHABASCA BITUMEN

by

M.V. Chandra Sekhar and Marten Ternan

Energy Research Laboratories
Department of Energy, Mines and Resources,
Ottawa, Ontario, K1A 0G1, Canada

When a hydrocracking process, rather than a coking process, is used to perform molecular weight reduction of bitumen from the Athabasca Oil Sands, the yield of usable liquid product is 10 to 15 per cent higher. However, the hydrocracking process also produces 5 to 10 per cent pitch boiling above 525°C. This pitch material contains high concentrations of sulphur, nickel, vanadium and iron. If it were burned large quantities of sulphur dioxide would be formed, probably necessitating a prohibitive investment for stack gas scrubbing. If it were used as a feedstock for a coking process a high yield of coke would be obtained. Coke containing large concentrations of sulphur and metals is not a desirable commodity. A third possibility would be gasification of the pitch. Unfortunately gasification processes are also capital intensive.

After some initial experiments at gasification conditions, it became apparent that pyrolysis of the pitch occurred at low temperatures. Both gaseous and liquid hydrocarbon products were formed. Therefore the pyrolysis of the pitch was investigated prior to studies on pitch gasification. By gaining an appreciation for pitch pyrolysis and gasification reactions it might be possible to find a better method of pitch utilization.

Experimental

A batch reaction system was used to study the rate of the pyrolysis reaction. Samples of pitch (100 mg) were placed in a cylindrical quartz basket (15 x 40 mm) which was suspended from the weighing mechanism of a Cahn RG electrobalance. A stream of helium (150 ml/min) flowed sequentially through the chamber containing the weighing mechanism, into the top of the hangdown tube containing the pitch sample and out of the bottom of the hangdown tube, through a condenser and into a gas sampling system. Volatile products from the pyrolysis reaction were carried by the helium stream through the condenser where the heavier components accumulated. The hangdown tube containing the pitch sample was surrounded by a tubular furnace. It could be operated either isothermally or in a temperature programmed mode using a Fisher Model 370 temperature programmer. Both the sample weight and the temperature of the interior of the hangdown tube were monitored continuously.

In order to obtain the quantities of product samples required for all the analyses, some experiments were performed with approximately 5-gram samples of the feedstock. These experiments were performed isothermally without the electrobalance mechanism attached to the sample basket.

Attempts were made to investigate possible heat and mass transfer limitations of the reaction rate. A series of experiments was performed in which the basket containing the pitch sample was disconnected from the electrobalance weighing mechanism so that a thermocouple could be placed into the centre of the pitch sample. The difference in temperature recorded by the thermocouple in the pitch and the one in the vapour space was always less than $5^{o}C$ regardless of the heating rate. Calculations indicated that the heat transfer rate sustained by this temperature difference was an order

of magnitude smaller than the heat transfer rate required to sustain the reaction rate. On this basis it was concluded that the rate of heat transfer to the pitch sample had a minor effect on the rate of the endothermic pyrolysis reaction. A second series of experiments was performed in which the length of the basket containing the pitch samples was varied by a factor of four. The purpose of these experiments was to increase the distance the pyrolysis product molecules would have to travel from the surface of the reaction mixture to the flowing helium carrier gas. No change in the rate of pyrolysis was observed with varying length of the basket, indicating that the reaction rate was not limited by bulk vapour phase mass transfer. Other experiments were performed in which the height (and therefore the quantity) of pitch in the quartz basket was varied. No change was observed in the measured quantities shown in Figure 1. This indicated that the reaction rate was not limited by diffusion of species within the reaction mixture.

The pyrolysis products were analyzed by several techniques. The Carle S-111-H gas chromatograph used for gas analysis contained four different columns in series. It included a palladium hydrogen transfer tube which permitted the hydrogen in the helium carrier gas to diffuse through a palladium membrane into a nitrogen stream. The hydrogen was then analyzed in the nitrogen carrier gas by a thermal conductivity detector. The other components remained in the helium carrier gas and were analyzed by a different thermal conductivity detector.

Elemental analysis, C^{13} n-m-r analysis, and chromatographic distillations were performed on the liquid phase pyrolysis products. The chromatographic distillation equipment included a Carlo Erba chromatograph and a Model SP4000 Spectra Physics data analyzer. The n-m-r analysis was

performed using a Varian model CFT-20 instrument. Elemental analyses were performed using standard ASTM methods.

The pitch used in these experiments was the portion of the liquid product boiling above 525°C, obtained by thermally hydrocracking Athabasca bitumen in a pilot-plant reactor. The Athabasca bitumen was obtained from Great Canadian Oil Sands Ltd., at Fort McMurray, Alberta. Properties of the hydrocracked pitch feedstock are shown in Table 1.

Results and Discussion

Typical experimental data from the microbalance reactor are shown in Figure 1. Each of the experiments was performed at a different heating rate. An example is shown in Figure 1C.

One simple representation of the pitch pyrolysis reaction is:

$$\text{PITCH} \longrightarrow \text{GAS} + \text{LIQUID} + \text{CHAR} \qquad 1)$$

The products can be classified at ambient conditions as gas phase material, distillable liquid, and non-distillable char. At any time during the course of the reaction the material in the microbalance reactor would be a combination of the incompletely reacted hydrocarbon originating from the pitch and the char reaction product. Belinko, Ciavaglia and Nandi (1) have recently obtained experimental evidence for the co-existence of these two substances at similar reaction conditions. This combination of incompletely reacted material and char will be referred to as the residue.

The weight of the residue is shown as a function of both time and temperature in Figure 1A. The temperature abscissa at the top of the figure has a linear scale above 250°C. Very little reaction occurred up to approximately 400°C. The greatest change in residue weight occurred between 400°C and 500°C. Above 500°C the rate of change in weight was small but relatively constant. In one experiment the sample was held at 900°C for 80 hours.

The residue weight was still changing at about 0.003 weight per cent per minute, even though the weight loss was approximately 65 per cent of the original sample.

The rate of change in weight of the residue with time is shown in Figure 1B. The initial low rate of the pyrolysis reaction was probably caused by the low temperature. As the temperature increased the reaction rate went through a maximum near 450°C and then declined. Eventually the reaction rate became quite small. This was probably caused by the increasing proportion of char and the decreasing proportion of reactive hydrocarbon in the residue.

When pyrolysis or volatilization experiments have been performed on other materials, curves having similar shapes have been observed. Flynn and Wall (2) analyzed polymeric materials extensively. Oil shales have been investigated by Granoff and Nuttall (3). Several studies (4,5,6) have been reported on coals.

Values illustrating product yields and gas composition from isothermal experiments are shown in Table 2. The yield data shown were obtained after a reaction time of 2 hours. The amount of liquid formed was approximately three times greater than the amount of gas formed. Although some of the material was not accounted for, the closure of the mass balance was acceptable for present purposes. It is interesting to compare the yield data in Table 2 with yields that might be anticipated from a coking process. Fuqua and Lahn (7) have reported yields from a commercial coking process for three feedstocks with Conradson Carbon Residue (CCR) values ranging from 13 to 34 wt %. Extrapolation to a CCR value of 65 might correspond to the pitch used in these studies. On this basis their gas yields would be higher and their liquid yields would be lower than those reported in Table 2.

The composition of the gas phase was virtually the same when isothermal experiments were performed at both 450 and 550°C. One surprising feature was the absence of any significant amount of olefinic material in the gas phase. Several chromatographic peaks corresponding to olefin gases were observed. However the amounts of these gases were minute. It is possible that any olefinic products formed could have been hydrogenated after reacting with hydrogen donor species. Alternatively the gas phase products could have originated as paraffinic side chains attached to larger structures, perhaps condensed aromatic or naphthenic rings.

The carbon 13 n-m-r spectra for the pitch feedstock and the liquid product are shown in Figure 3. The broad peak on the left between 100 and 200 represents aromatic carbon atoms. The sharp peaks on the extreme right represent non-aromatic atoms. The three sharp peaks in the centre were caused by the $CDCl_3$ solvent. The feedstock contained 67 per cent aromatic carbon atoms, compared to 38 per cent in the liquid product.

The liquid product analyses are shown in Figure 2 and in Table 1. Figure 2 shows the results of a chromatographic distillation. It is apparent that the distribution of material as a function of boiling point is almost linear up to 500°C. It is possible that the liquid sample may have contained some very high molecular weight material which would have remained on the chromatographic column and would not have been detected. The elemental analyses in Table 1 indicated that the liquid product contains less sulphur and nitrogen than the feedstock. Furthermore the hydrogen-to-carbon ratio in the product (1.3) is significantly higher than that in the feedstock (1.0).

The hydrogen-to-carbon atomic ratio in the residue was found to be a linear function of the residue weight, as shown in Figure 4A. The weight per cent hydrogen in the residue, obtained on an ash free basis is related to the residue weight in Figure 4B. The data points were obtained at different temperatures and different reaction times. These data clearly

indicate that as the reaction proceeds the residue becomes progressively more depleted in hydrogen. This is consistent with the gaseous product and the liquid product having hydrogen-to-carbon ratios greater than the feedstock. The pyrolysis reaction can therefore be considered to have gone to completion when the hydrogen content of the residue reaches zero.

In analyzing the reaction rate data, it is important to consider the composition of the reactant. The initial reactant, pitch, is a complex mixture of many molecular species. In a batch reaction system like the one used in this study, the composition of the reactant will change continuously. Figure 4 provides evidence for this statement. The reaction rate can be expected to change as the composition of the reactant changes. To eliminate this variable, the reaction rate data were analyzed at specific values of reactant composition.

The amount of residue in the reaction system is an indication of the reactant composition as shown in Figure 4. Therefore the rate of change in residue weight and the temperature are shown as functions of the amount of residue in Figure 5. The data are shown for four of the eight different heating rates used. The faster heating rates produced higher temperatures and greater reaction rates for any given amount of residue. With this representation it is easy to compare reaction rates at constant amount of residue (constant reactant composition).

The reaction rate data have been analyzed in terms of Equation 1. The char was assigned a hydrogen-to-carbon ratio of zero and the pitch was assigned the value of the intercept (1.013) in Figure 4A. In order to simplify the analysis the residue was assumed to consist of two components, unreactive char and reactive pitch. Therefore, as the reaction proceeded along the abscissa in Figure 4, the amount of char would increase and the amount of pitch would decrease. This assumption accounts for the decreasing

reactivity of the residue as the reaction proceeds. Although this assumption is convenient, it may be somewhat inaccurate, in that the reactive portion of the residue is a mixture which differs from the initial pitch composition.

Proceeding with the above assumption and being as general as possible, the pyrolysis of pitch can be written as a nth order reaction

$$\frac{-dW_P}{dt} = kW_P^n \qquad 2)$$

where W_P is the weight of pitch present in the reaction system expressed as a percentage of the original sample weight, and k is the rate constant. The Arrhenius equation,

$$k = A \exp(-E_a/RT) \qquad 3)$$

where A is the Arrhenius constant, E_a is the activation energy, R is the gas constant and T is the temperature, can be substituted in Equation 2 and logarithms taken to obtain

$$\ln\left(\frac{-dW_P}{dt}\right) = \ln A - \frac{E_a}{RT} + n \ln W_P \qquad 4)$$

W_P can be expressed in terms of W_R, the weight of residue in the reaction system expressed as a percentage of the original sample weight, by solving the following three equations in three unknowns. The total material balance is

$$W_R = W_P + W_C \qquad 5)$$

where W_C is the weight of char in the reaction system expressed as a percentage of the original sample weight.

The hydrogen component material balance can be written as

$$W_R Y_R = W_P Y_P + W_C Y_C \qquad 6)$$

where Y_R, Y_P and Y_C are the weight per cent hydrogen on an ash-free basis in the residue, the unreacted pitch and the char respectively. The experimentally determined relationship between W_R and Y_R represented by the straight line in Figure 4B yields the equation,

$$Y_R = 0.106\ W_R - 3.36 \qquad 7)$$

Values for $Y_P = 7.24$ and $Y_C = 0.0$ were obtained from the intercepts in Figure 4B. Substitution of Equation 7 and the values of Y_P and Y_C into Equation 6 produces,

$$W_P = 0.0146\ W_R^2 - 0.464\ W_R \qquad 8)$$

This can be differentiated to obtain

$$\frac{dW_P}{dt} = (\ 0.0293\ W_R - 0.464\ )\ \frac{dW_R}{dt} \qquad 9)$$

Equations 8 and 9 can now be used to obtain dW_p/dt from the experimentally determined weight loss rates. This has been done in Figure 5 where both dW_p/dt and T are shown as a function of W_R. The four curves shown in Figure 5 are typical of the eight sets of experimental results.

These data were used to obtain values for both the activation energy and the pre-exponential factor. Equation 4 can be rearranged to obtain

$$\ln\ (-\frac{dW_P}{dt}) = I - \frac{E_a}{RT} \qquad 10)$$

where

$$I = \ln A + n \ln W_P \qquad 11)$$

The value of I will be a constant provided W_P is constant. According to Equation 8, W_P will be a constant when W_R is constant. Therefore Equation 10 can be used to analyze the rate data if W_R is held constant. This was accomplished by taking specific values of dW_P/dt and T corresponding to a specific value of W_R in Figure 5 and plotting them in Figure 6. The data for each value of W_R produced a different straight line, from which values for E_a and I were obtained. Each of the three lines shown as examples in Figure 6 represents respectively a value for W_R where the rate was increasing (98.5%) approaching its maximum (80%) and decreasing (65%).

Equation 11 suggests a linear relationship between the intercept I and ~~Wp~~ $\ln W_p$. However when a linear regression between these two variables was attempted, a poor correlation was obtained indicating perhaps the Arrhenius factor A and the order n are not constants through the course of the pyrolysis.

It is also apparent from Figure 6 that both the activation energy, E_a and the intercept, I, do not remain constant through the course of the pyrolysis. The activation energy increases initially as the extent of reaction increases, and approaches a maximum when about 20% of the sample has decomposed. During the course of the remainder of the pyrolysis the activation energy was found to be decreasing with increasing reaction. The intercept I, which includes the Arrhenius constant A, was also found to exhibit a similar pattern of behaviour. This suggested the existence of a compensation effect between intercept and the activation energy, as shown in Figure 7. The data points on the top and bottom compensation lines represent values of W_R for which the reaction rate was increasing and decreasing respectively.

As W_R decreased values of E_a and I increased along the upper compensation line in the direction of the top right hand corner of the figure. For values of W_R close to the maximum reaction rates, there was a transition from the upper to the lower compensation line. As W_R continued to decrease values of E_a and I decreased along the lower compensation line toward the bottom left hand corner of the figure. The observation of two parallel compensation lines is not unique to this study. Multiple compensation lines have been observed in other reactions such as the decomposition of hydrogen peroxide (8).

The compensation effect has normally been observed when reaction studies have been performed using different catalysts. Ranganathan, Bakhshi and Mathews (8) explained the compensation effect which they observed in terms of the different bulk and surface properties of their catalysts. Explaining the compensation effect in terms of catalyst properties may be inappropriate in this case, since no synthetic catalysts were added in these pyrolysis studies. However the mineral matter present in the pitch may have acted as a natural catalyst.

Alternatively it is possible to hypothesize that the compensation effect observed in these studies may have been related to the varying composition of the hydrocarbons in the pitch. It is reasonable to presume that the lowest strength bonds would be broken first and that they would correspond to the lowest activation energy. On this basis the activation energy would be expected to increase continuously as the reaction proceeds (that is as W_R decreases). This could explain the upper compensation line. No really satisfactory explanations for the lower compensation line are obvious at the present time.

The compensation effect has also been observed during coal char gasification reactions (9). In principle pyrolysis reactions could occur at typical commercial gasification conditions. However if pyrolysis products were formed they would probably react very quickly with the oxygen, steam or carbon dioxide present. It is tempting to suggest that the compensation effect in coal char gasification may be related to the compensation effect we have observed during pyrolysis of pitch.

Pulsifer and co-workers (10) have suggested that the amount and nature of coal ash may be responsible for the compensation effect in coal char gasification in the same way that varying catalyst properties are responsible for the compensation effect in other reactions. While this is undoubtedly correct, differences in the hydrocarbon composition (coal macerals) may also have had some influence on the compensation effect in coal char, similar to the one we have observed for pyrolysis of pitch.

The compensation effect is usually expressed as

$$\ln A = a + bE \qquad (12)$$

where $a = \ln k_{iso}$, $b = 1/RT_{iso}$, k_{iso} is the iso-kinetic rate constant and T_{iso} is the iso-kinetic temperature. As a result both a and b are constants. Equation 12 was substituted into Equation 11 to give

$$I = a + bE + n \ln W_P \qquad 13)$$

A multiple linear regression on Equation 13 was then performed to obtain values of a, b and n. Such an analysis for the upper line in Figure 7 produced values of a = 4.307, b = 0.742 and n = 1.050. This suggests that this portion of the pyrolysis can be best explained by first order kinetics. The iso-kinetic temperature under these conditions corresponds to 680°K. These results are graphically shown in Figure 8.

A similar regression analysis on the lower compensation line of Figure 7 yields results that cannot be explained on physical grounds. The value obtained for n, the reaction order did not appear to represent any imaginable process. When the data were analyzed in terms of several diffusion models (11) no satisfactory correlations were obtained. It may be that the postulated reaction, Equation 1, is too simple. During the course of the pyrolysis reaction, the residue undoubtedly contains many species in addition to the reactant (pitch) and solid product (char). It may be necessary to account for the reaction intermediates in order to explain the lower line in Figure 7.

The data presented in this paper indicate the importance of the pyrolytic reactions, the bulk of which occur at temperatures below 500°C. As much as 35% by weight of the original sample was found to decompose into volatile liquid and gaseous products at these temperatures. The liquid products are richer in hydrogen and low in aromatic content compared to the unreacted pitch. Above 500°C, the rate of decomposition is slower and gradually decreases with time. There appears to be at least two stages in the overall

decomposition. During the first stage the activation energy is increasing with the extent of reaction, approaching a maximum when about 20% of the sample has decomposed. Under these conditions, the pyrolysis was found to follow first order kinetics with respect to the unreacted pitch. The activation energy and the pre-exponential factor, which were found to be functions of the extent of decomposition, exhibit a well defined compensation effect. During the second stage the activation energy decreases with increasing extent of reaction. The kinetics of the pyrolysis under these conditions become more complex and are not well understood.

ACKNOWLEDGEMENTS

The authors greatly appreciate the assistance of Mr. M. Channing in performing the experiments, Mr. R. Ozubko in performing the carbon 13 n-m-r analyses, Mr. G. Lett for measuring the hydrogen-to-carbon ratios and Mr. R. Gill for distilling the liquid products.

REFERENCES

1. K. Belinko, L.A. Ciavaglia, and B.N. Nandi, Energy Research Laboratories Report 77-95(R).

2. J.H. Flynn and L.A. Wall, J. Res. Nat. Bur. Stand., A 70, 487 (1966).

3. B. Granoff and H.E. Nuttall Jr., Fuel, 56, 234 (1977).

4. M.G. Skylar, V.I. Shustikov and I.V. Virozub, Int. Chem. Eng., 9, 995 (1969).

5. W.H. Wiser, G.R. Hill and N.J. Kertamus, Ind. Eng. Chem. Process Des. Develop., 6, 133 (1967).

6. O.P. Mahajan, A. Tomita and P.L. Walker, Jr., Fuel, 55, 63 (1976).

7. B.B. Fuqua and G.C. Lahn, "Flexicoking for Heavy Crude Upgrading", International Petroleum Exposition, Tulsa, Oklahoma (1976).

8. R. Ranganathan, N.N. Bakhshi and J.F. Mathews, Can J. Chem. Eng. 55, 544 (1977)

9. P.L. Walker, Jr., M. Shelef and R.A. Anderson, in Chemistry and Physics of Carbon (ed. P.L. Walker, Jr.) vol.4, p.287. Marcel Dekker, New York (1968).

10. P.P. Feistel, K.H. Van Heek, H. Juntgen and A.H. Pulsifer, Carbon, 14, 363 (1976).

11. J. Crank, The Mathematics of Diffusion, Clarendon Press, Oxford, 1956.

CAPTIONS FOR FIGURES

Figure 1 Amount of Residue (Wt %), $-\Delta W_R/\Delta t$ (Wt % Residue per Min), and Temperature (^{o}C) versus Time (Min)

Figure 2 Cumulative Volume Percent Liquid Distilled versus Boiling Point (^{o}C).

Figure 3 Carbon 13 n-m-r Spectra for the Pitch Feedstock (bottom) and for the Liquid Product (top).

Figure 4 Hydrogen-to-Carbon Atomic Ratio and Hydrogen Weight Per cent (daf) versus Amount of Residue (Weight Per cent).

Figure 5 Rate of Change of Amount of Pitch $-\Delta W_P/\Delta t$ (Weight Per cent per Min), and Temperature (^{o}C) versus Amount of Residue, W_R, (Weight Percent). Heating rates were 2.5, 5, 10 and 20^{o}C per minute for curves 1,2,3 and 4 respectively.

Figure 6 Natural Logarithm of $-\Delta W_p/\Delta t$ versus Inverse Temperature ($^{o}K^{-1}$). Squares, circles and triangles represent values for W_R of 98.5, 80 and 65 Per cent respectively.

Figure 7 I (Intercept) versus Activation Energy (kJ/mole).

Figure 8 ln A versus Activation Energy (kJ/mole).

TABLE I

FEEDSTOCK AND PRODUCT PROPERTIES

	Pitch	Liquid Product
Proximate Analysis, wt %		
Moisture	nil	
Ash	5.2	
Volatile Matter	42.4	
Fixed Carbon (by diff.)	52.4	
Ultimate Analysis, wt %		
Carbon	79.6	81.9
Hydrogen	6.8	9.0
Sulphur	5.4	4.5
Nitrogen	1.5	0.6
Ash	5.2	nil
Oxygen (by diff.)	1.5	
Pentane Insolubles, wt %	70.1	
Benzene Insolubles, wt %	27.1	
Conradson Carbon Residue, wt %	63.5	
Tetrahydrofuran Insolubles, wt %	10.4	
Ash Analysis, wt %		
SiO_2	43.3	
Al_2O_3	24.7	
Fe_2O_3	11.4	
Mn_3O_4	0.3	
TiO_2	6.6	
P_2O_5	0.3	
CaO	2.8	
MgO	1.6	
SO_3	1.2	
Na_2O	0.2	
K_2O	1.7	
V_2O_5	3.1	
NiO	0.8	

TABLE 2

PRODUCT DISTRIBUTION AND GAS ANALYSIS

Reaction Temperature, °C	450	550
Residue, wt %	73	66
Liquid, wt %	17	21
Gas, wt %	6	6
Unaccounted, wt %	4	7
Gas Analysis (vol %)		
H_2	21	
H_2S	11	
methane	1	
C2	20	
C3	23	
C4	17	
C5	6	
C6	1	

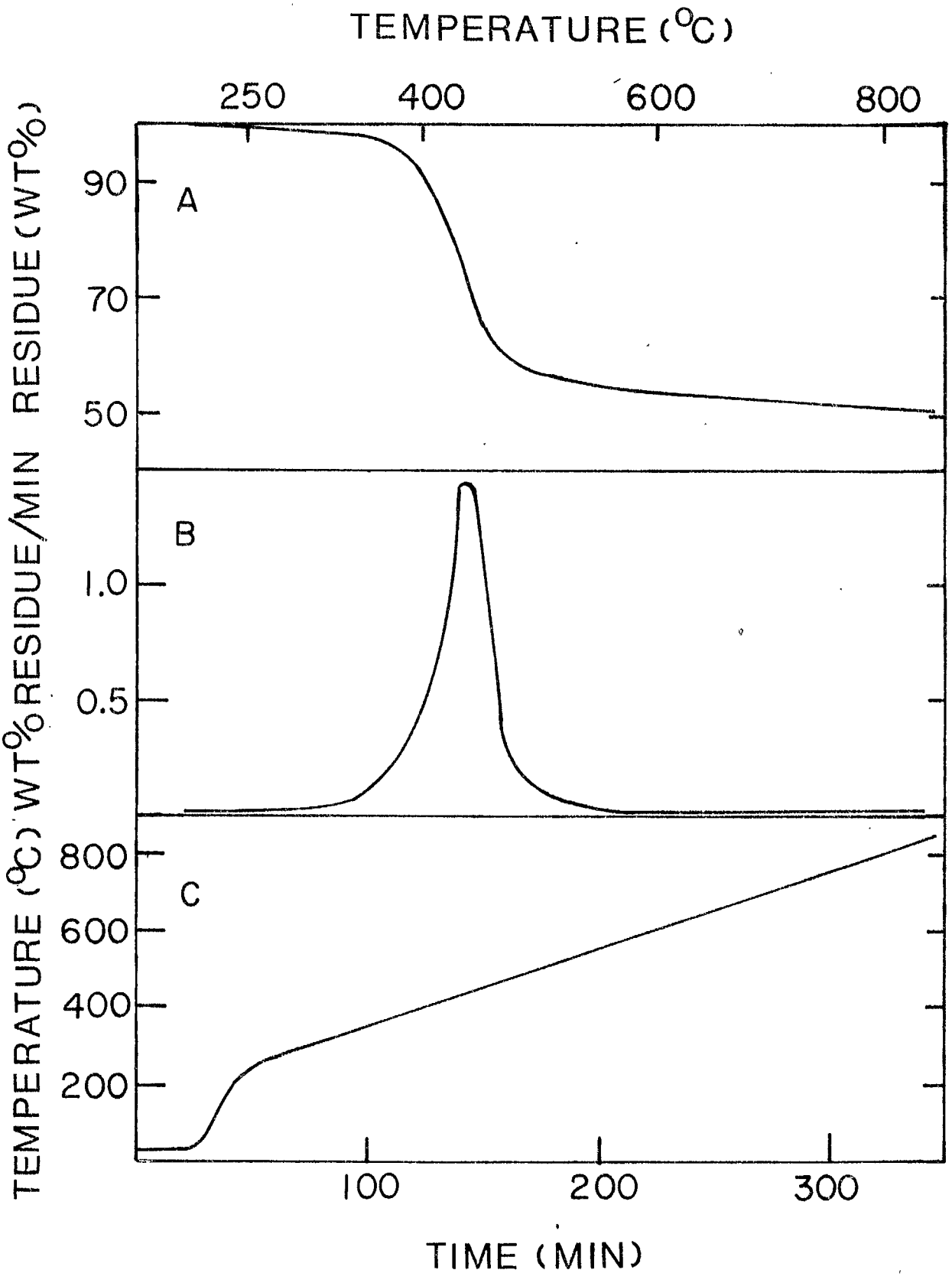

Figure 1

Fig. 1

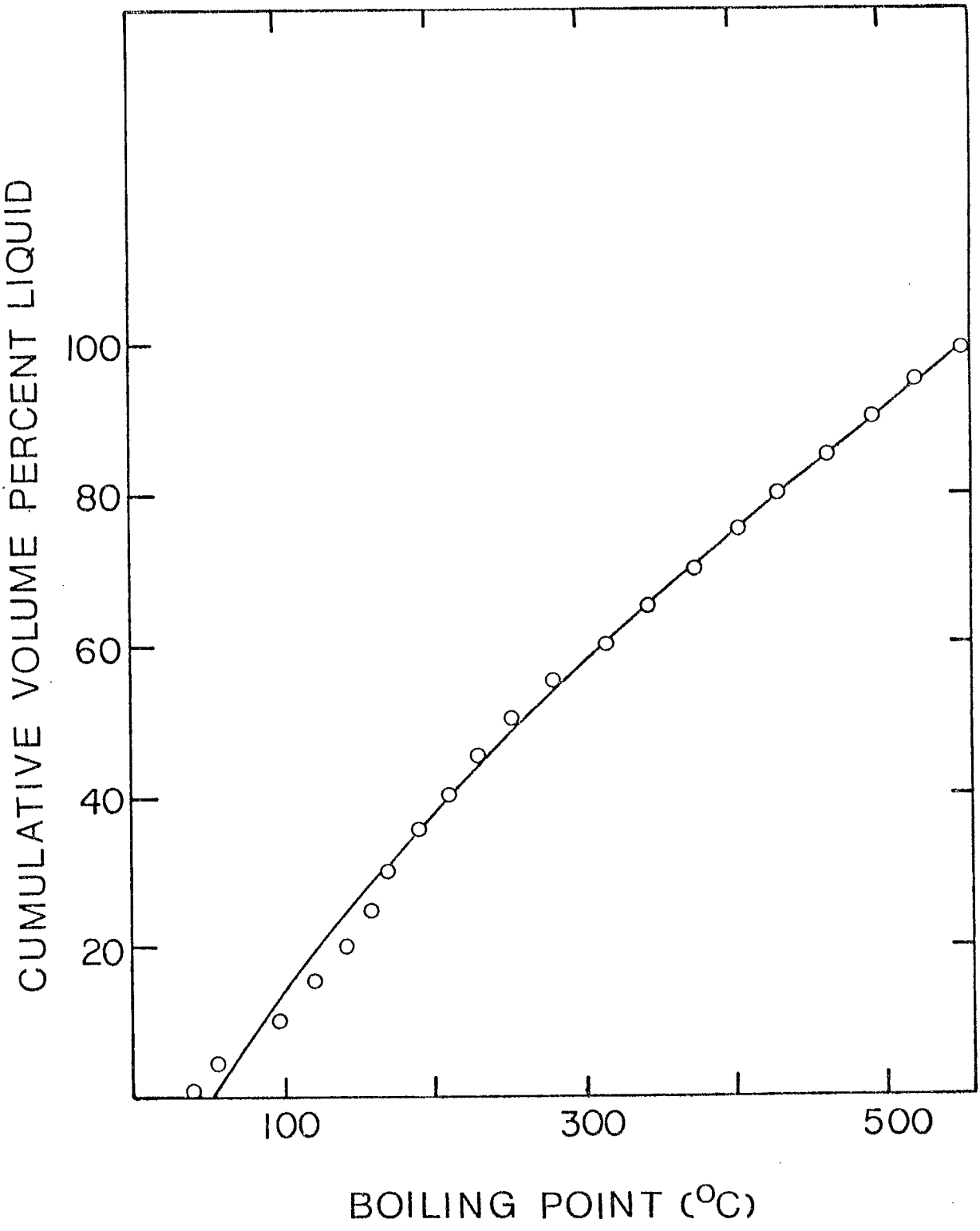
CUMULATIVE VOLUME PERCENT LIQUID
100
80
60
40
20
100
300
500
BOILING POINT (°C)

Figure 2

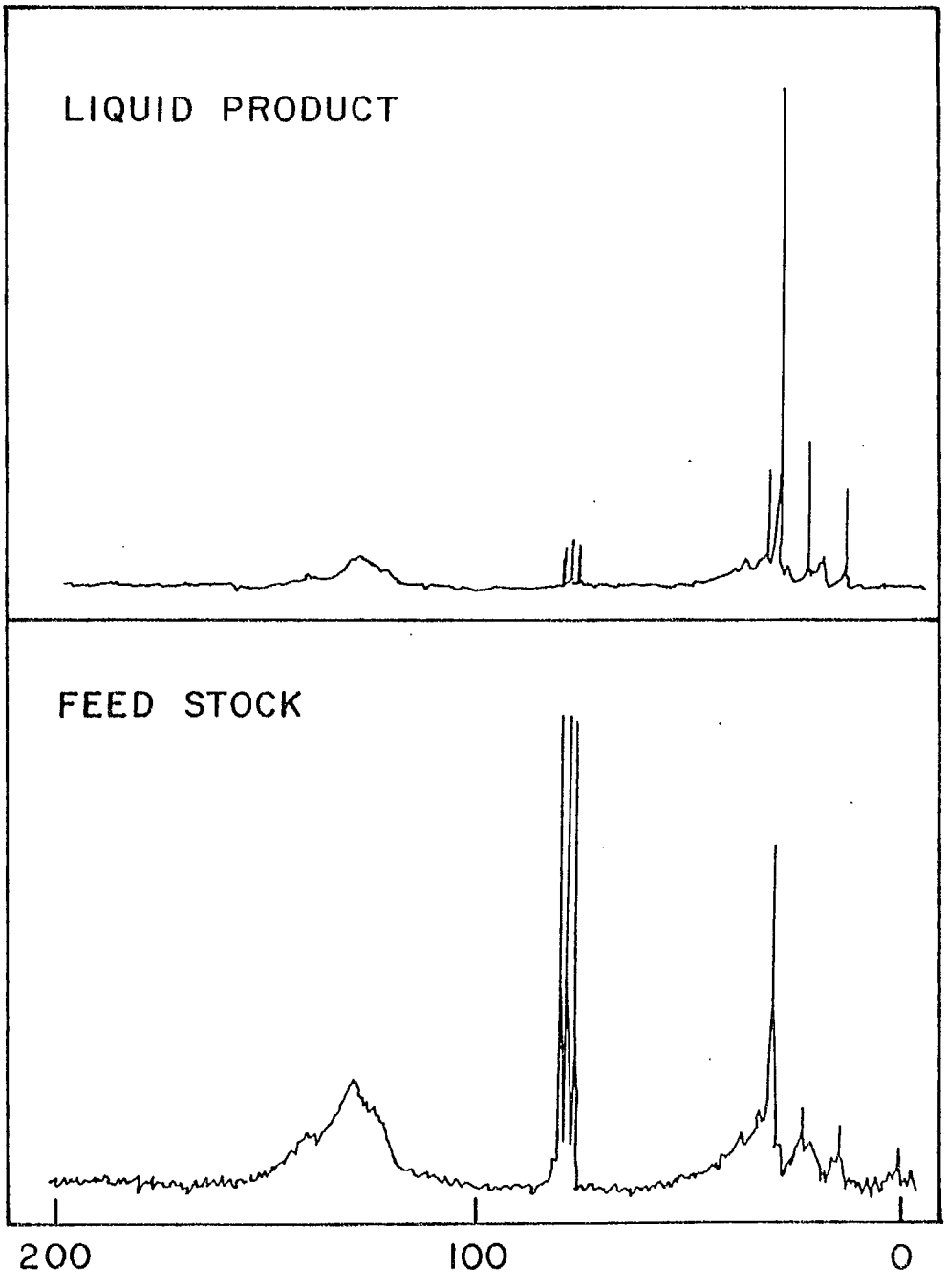

Figure 3

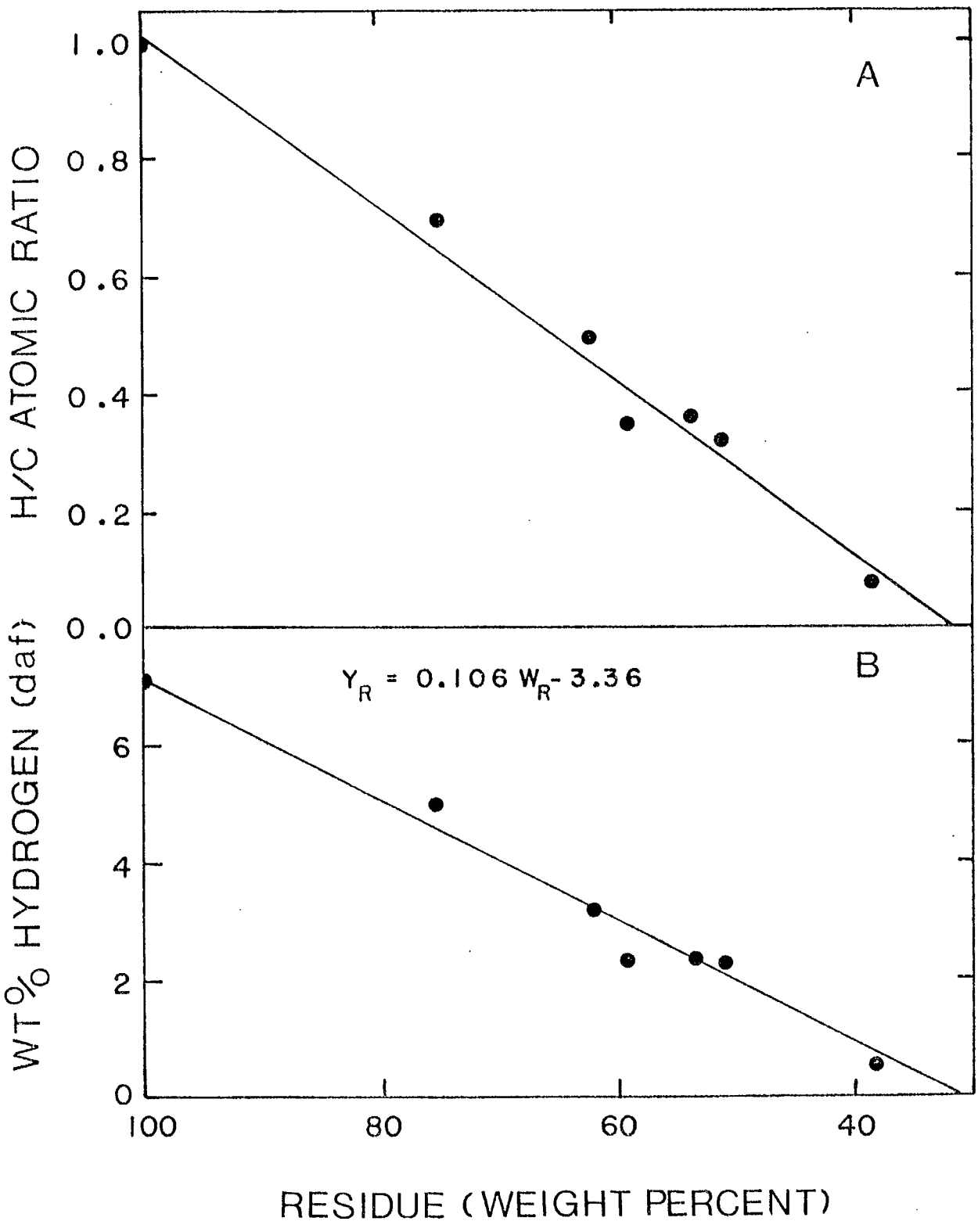
A
B
H/C ATOMIC RATIO
WT% HYDROGEN (daf)
$Y_R = 0.106\ W_R - 3.36$
1.0
0.8
0.6
0.4
0.2
0.0
6
4
2
0
100
80
60
40
RESIDUE (WEIGHT PERCENT)

Figure 4

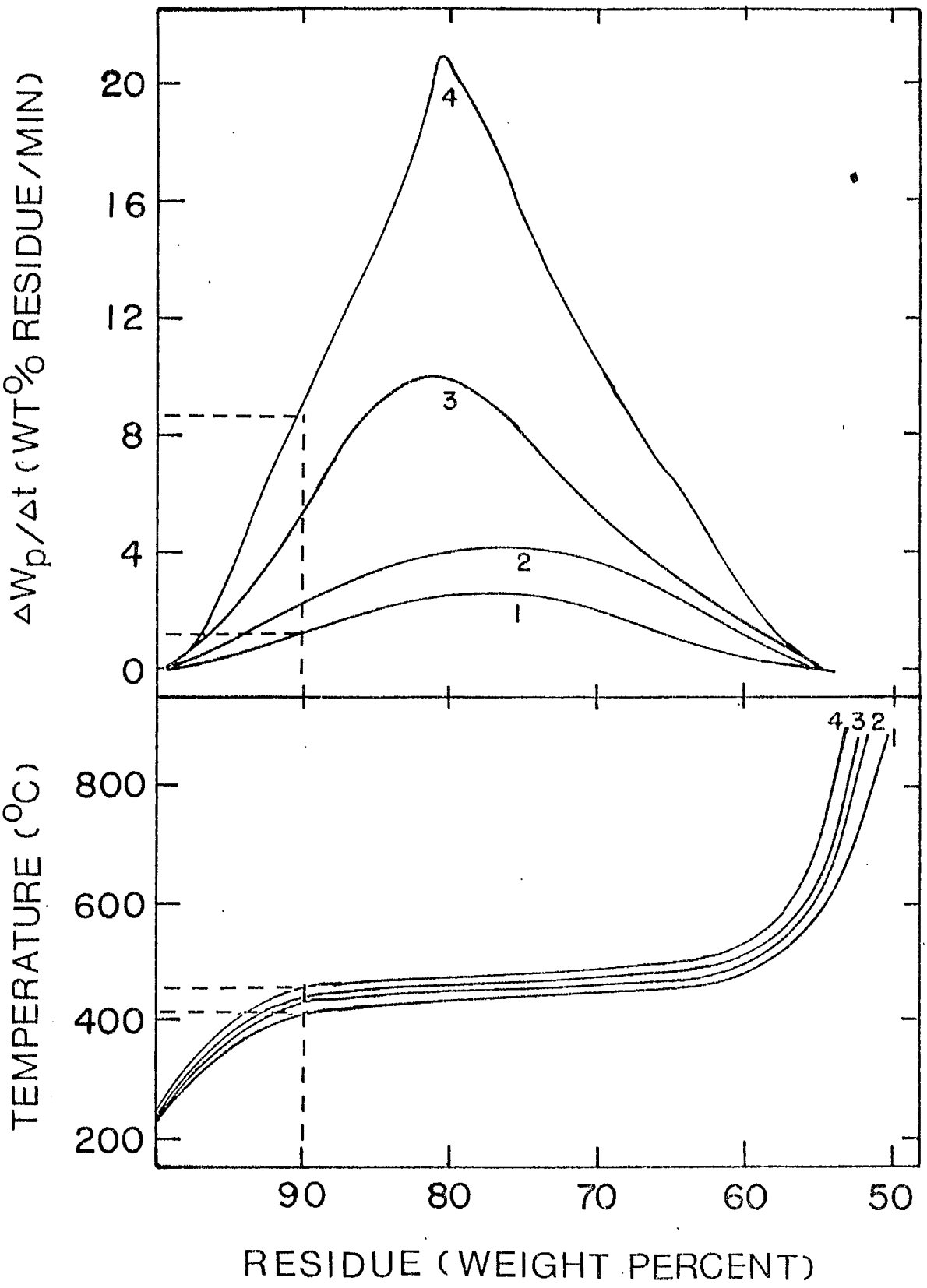
20
16
12
8
4
0
$\Delta W_p/\Delta t$ (WT% RESIDUE/MIN)
4
3
2
1
800
600
400
200
TEMPERATURE (°C)
4 3 2 1
90
80
70
60
50
RESIDUE (WEIGHT PERCENT)

Figure 5

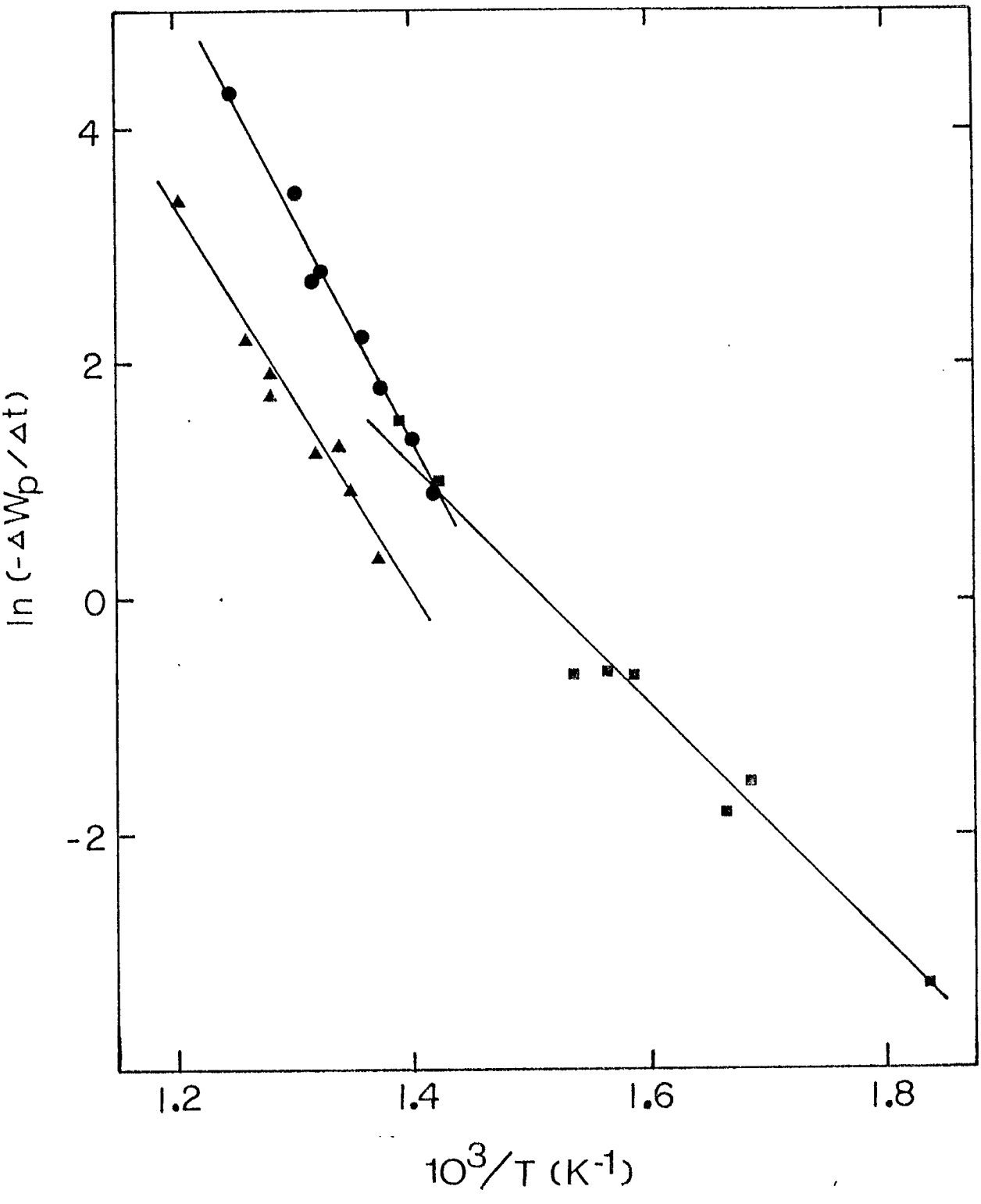

Figure 6

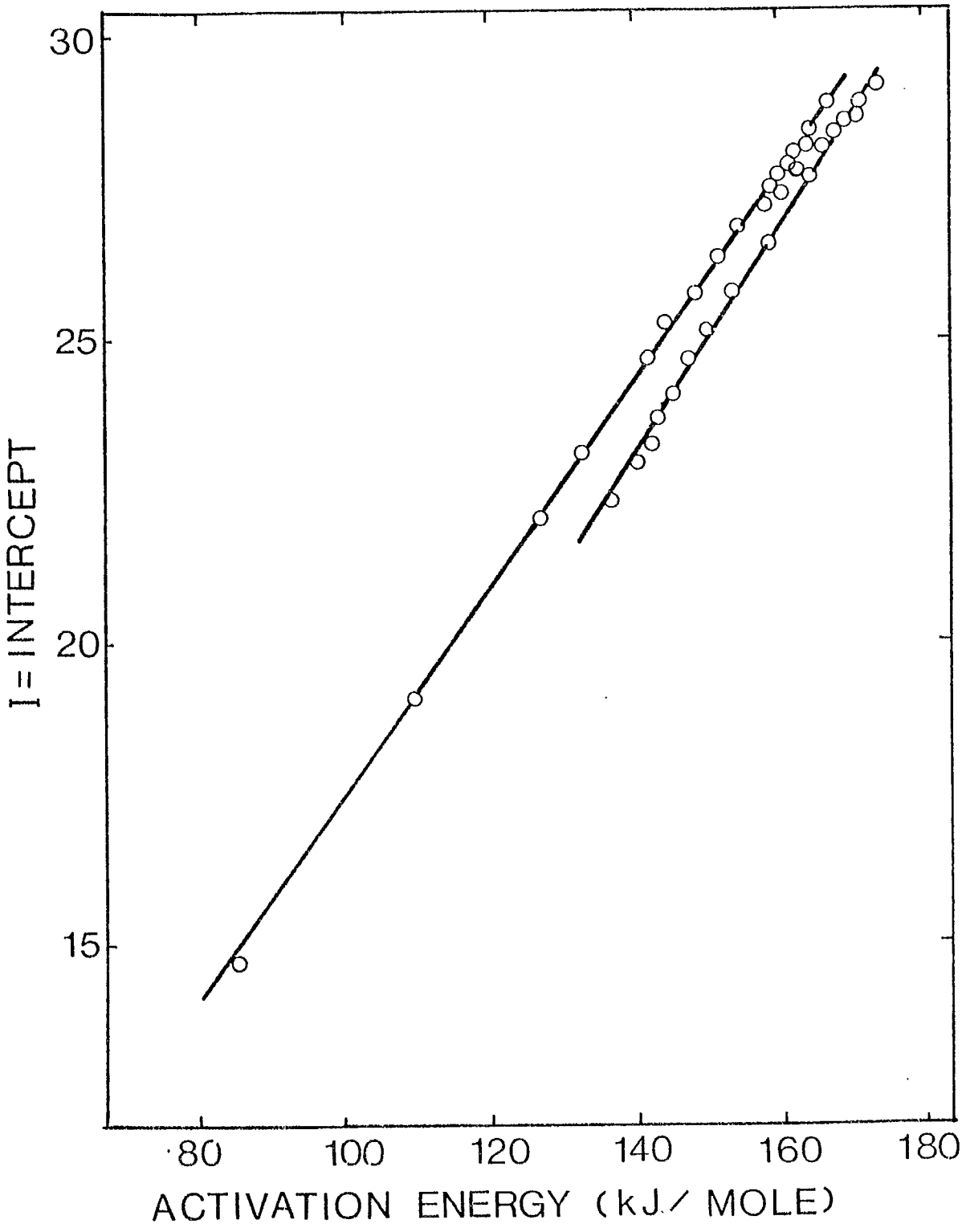
30
25
20
15
I= INTERCEPT
80
100
120
140
160
180
ACTIVATION ENERGY (kJ/ MOLE)

Figure 1

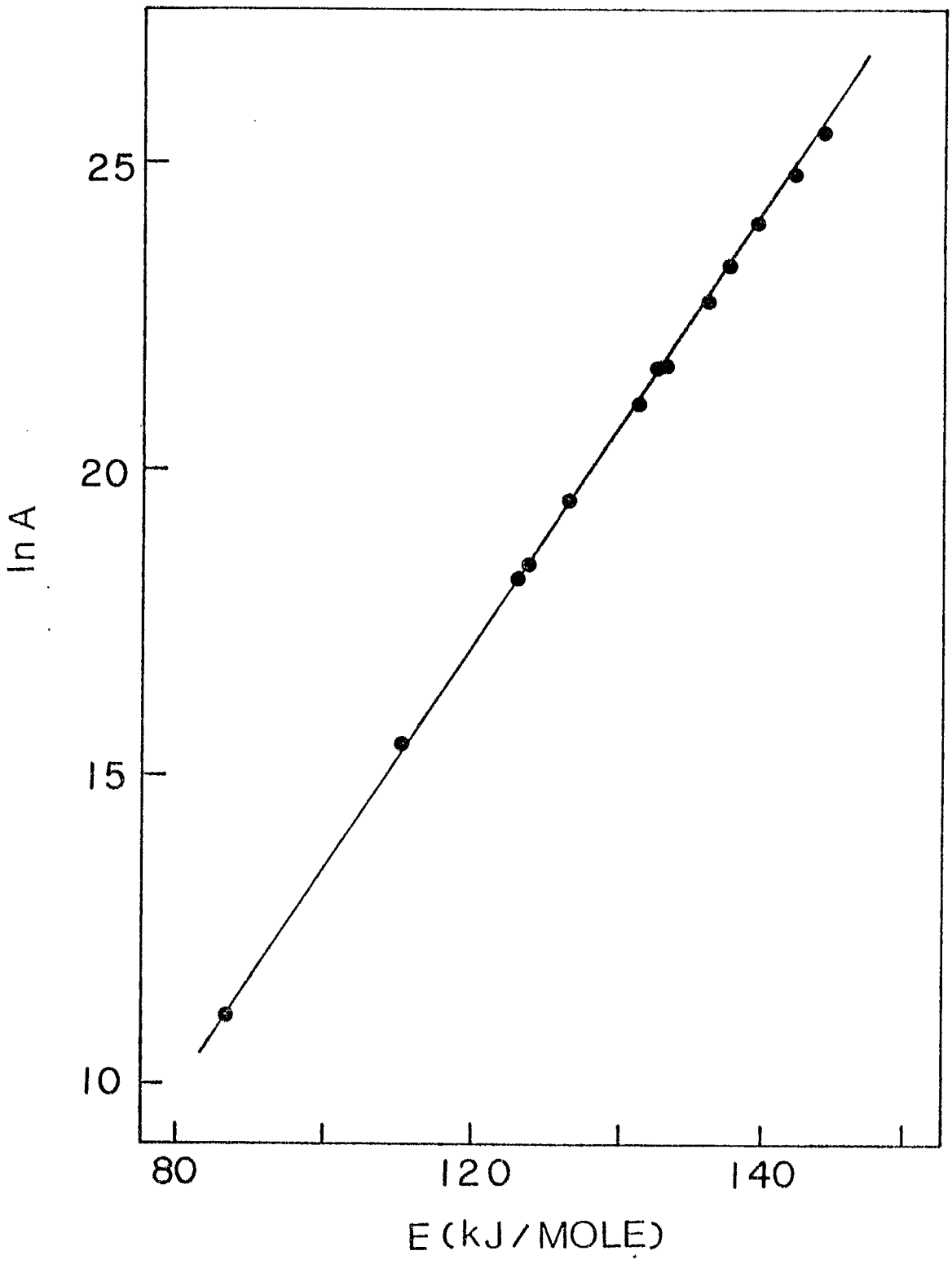

Figure 8